Journal of Luminescence 51 (1992) 39–50
North-Holland

JOURNAL OF
LUMINESCENCE

Studies of crystalline aggregates of pheophorbide and bacteriopheophorbide by electro-absorption (Stark effect) spectroscopy and powder X-ray diffraction

David S. Gottfried and Steven G. Boxer
Department of Chemistry, Stanford University, Stanford, CA 94305-5080, USA

Received 25 June 1991
Revised 21 August 1991

Absorption and electro-absorption (Stark effect) spectra of polycrystalline and lyophillized samples of pheophorbides and bacteriopheophorbides have been measured in order to obtain information on the consequences of intermolecular interactions on electronic structure. The results support the general hypothesis that large red shifts in the absorption spectra of photosynthetic aggregates are associated with increased dipolar character in the excited state due to mixing with intermolecular charge transfer states. In some cases, new bands, which are difficult to detect or absent in the absorption spectrum, are observed in the electro-absorption spectrum, and these may be charge-transfer transitions. The structures of several polycrystalline aggregates, either ground single crystals or lyophillized powders, were analyzed by powder X-ray diffraction. In some cases, the powder diffraction of lyophyllized powders was found to be nearly identical to that predicted from single crystal diffraction data on the same chromophore. High quality electro-absorption spectra were also obtained and analyzed for the monomeric pigments.

1. Introduction

Many aspects of the initial photophysics and photochemistry of photosynthesis are the consequence of specific inter-chromophore interactions. These include rapid energy transfer in the antenna complexes and the initial electron transfer reactions in the reaction center. Intermolecular interactions among the photosynthetic chromophores result in spectroscopic changes relative to the isolated monomeric molecules that include red shifts of absorption bands (the Q_y band in particular) and inter-transition intensity borrowing. There has been a considerable effort in recent years to calculate both the spectroscopic (e.g. absorption, emission, circular dichroism, electro-absorption) [1–7] and dynamic (e.g. electron and energy transfer) [8–11] properties of photosynthetic arrays. Most attempts to simulate the energies and amplitudes of absorption and circular dichroism spectra begin with classical exciton theory [12,13]. Early calculations were generally limited to a treatment of dipole–dipole interactions between the lowest energy Q_y transitions and usually failed to simulate the magnitude of the red shifts as well as other observations [14]. More sophisticated methods have been developed to account for interactions of the Q_y transitions with higher energy transitions (Q_x and B), charge-transfer (CT) interactions, and orbital overlap [5,15]. These methods require precise geometric and structural information and are limited by the inadequate structural data available for many of the systems of interest. Even for bacterial reaction center (RC) complexes, whose structures are available [16–20], the precision is currently rather poor. Thus, precise information on intermolecular distances, as well as more subtle factors such as side-chain orientations and ring pucker [21] which may be important, is not yet available at the level needed for accurate calculations.

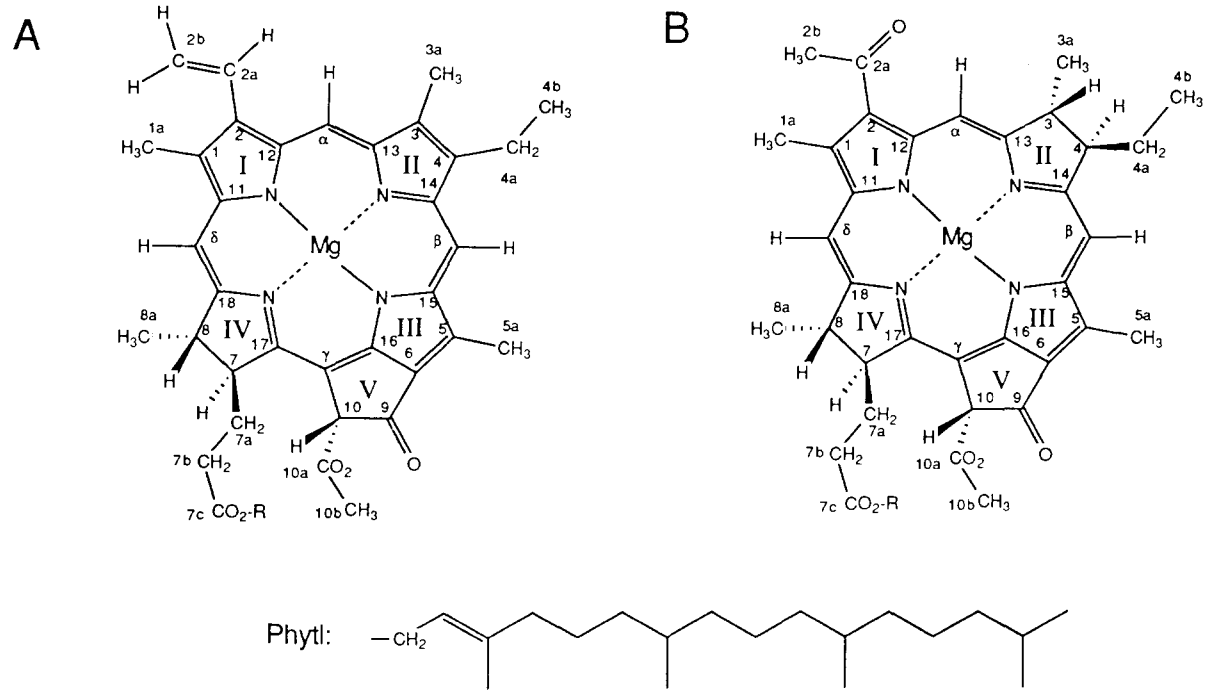

Fig. 1. Structure and numbering system for the macrocycles discussed in this paper. (A) Chlorophyll a; (B) bacteriochlorophyll a. R = $-CH_3$ in the methyl esters; Mg is replaced by 2 H in the pheophorbides; and $-CO_2CH_3$ group at position 10 is replaced with –H in the pyro-compounds.

In order to better interpret spectroscopic results for protein/chromophore systems, it would be advantageous to examine well-ordered, simple molecular aggregates. Although very few crystal structure determinations have been reported for chlorophylls (Chls) and bacteriochlorophylls (BChls), high resolution single crystal X-ray structures have been determined for methyl pheophorbide a (MePhide a) [22] and methyl bacteriopheophorbide a (MeBacPhide a) [23,24]. These are the focus of the present study (see fig. 1 for molecular structures). Earlier studies of the electronic absorption spectrum of MeBacPhide a single crystals [25] and simulations of these results [5] will be discussed in the context of the present work.

One of the objectives of this study is the examination of the role of structure on electronic excited state electro-optic properties (e.g. dipole moments) and their manifestation in the absorption spectrum. In particular, because of the large intermolecular interactions in these aggregates, charge transfer transitions, corresponding (in the simplest view) to a one electron oxidation and reduction between neighboring chromophores, are expected to be close in energy to locally excited $\pi\pi^*$ or exciton transitions [5,26,27]. Direct detection of pure CT bands is often difficult as they are expected to possess low oscillator strengths and may have broad line widths. In this preliminary study, we have attempted to detect CT transitions and the admixture of CT character in other transitions using applied electric fields (electro-absorption spectroscopy, often called Stark effect, electrochromism or electromodulation spectroscopy). This approach is based on the expectation that such transitions will have preferentially enhanced electric field effects. Such effects have been previously observed in electro-absorption studies of reaction centers [28–32], antenna complexes [33], and synthetic chlorophyll dimers [34–36]. In addition, electric fields have been used to assign exciton and CT transitions in single crystals and polycrystalline films of aro-

matic hydrocarbons [37–40] and phthalocyanines [41], and there have been extensive theoretical discussions of these transitions [54].

2. Materials and methods

2.1. Sample preparation

Methyl pheophorbide a, pyromethylpheophorbide a (pyroMePhide a) and methyl bacteriopheophorbide a were prepared according to established procedures [42,43]. Purity was assessed by thin layer chromatography, UV-visible absorption and NMR spectroscopy. PyroMePhide a and MePhide a were crystallized from 1 : 1 mixtures of $MeOH/CH_2Cl_2$ and benzene/MeOH, respectively. MeBacPhide a crystals were grown from CH_2Cl_2/benzene as described in ref. [24]. Lyophilized powders of the chromophores were prepared by freezing a benzene solution of the sample and pumping off the solvent leaving a fine powder.

Films of solid samples were prepared as follows. Small amounts of water-insoluble material (polycrystalline or lyophyllized powder) were ground using an agate mortar and pestle along with a suitable quantity of powdered poly(vinyl alcohol) [(PVA), 88% hydrolyzed, 125 000 MW], a water soluble polymer. A small amount of liquid nitrogen was usually added during the grinding to prevent thermal damage of the sample and to maintain hardness. The finely ground powder consisting of sample and PVA was then dissolved in 0.01% aqueous lauryl dimethyl-amine-N-oxide (LDAO) at 50°C giving a suspension of microcrystals which was poured onto a clean glass slide to form a thin film when dry (LDAO was added because it facilitates removal of the film from the slide). Films were typically 50–100 μm thick, and microscopic examination indicated that no sample particles larger than 20 μm in diameter were present. Poly(methyl methacrylate) (PMMA) films of the monomeric compounds were prepared as previously described [28,29].

2.2. Powder X-ray diffraction

X-ray diffraction of lyophyllized powders and ground polycrystalline samples was performed using one of two diffraction instruments: a Picker 4-circle diffractometer with a Rigaku X-ray generator (36 kV/16 mA) or a Scintag diffractometer (45 kV/40 mA) kindly made available by Dr. Lawrence Bernstein at Scintag, Inc. Scans of $2\theta = 2°–50°$ with 0.05° step size, 1° resolution, and 10 s dwell time were run under computer control. When single crystal structural data are available (for MePhide a and MeBacPhide a), computer simulations of the expected powder patterns are generated with standard programs using the atomic coordinates and thermal parameters. Using pre-determined diffraction and absorption terms for the atoms involved, this gives simulated intensity and angle values for all of the allowed reflecting planes. The stick pattern is then convolved with a Gaussian line shape to produce the patterns shown below. Powder X-ray diffraction of a PVA film containing lyophyllized MePhide a was also done to confirm that local structure in the aggregate is retained in the polymer film.

2.3. Electro-absorption spectroscopy

Electro-absorption spectroscopy was performed using the apparatus described elsewhere [35]. PVA films of the lyophyllized powder or polycrystalline samples and PMMA films of the monomeric compounds were coated with semi-transparent layers of Ni (typically 75 Å) on each side. All spectra were taken at 77 K.

In general, within the classical model of electro-absorption [44,45], the change in absorption, ΔA, upon application of an external electric field is comprised of contributions from the zeroth, first and second derivatives of the absorption spectrum. These terms arise from contributions due to changes in the oscillator strength, polarizability and dipole moment, respectively. With sufficiently accurate absorption and electro-absorption data, a fit of the ΔA data gives each contribution; however, in the present preliminary study, we only consider contributions due to changes in the dipole moment. In this case, the change in absorption in an applied electric field $\boldsymbol{F}_{\mathrm{ext}}$ for an isotropic sample can be described as:

$$\Delta A = \frac{C_\chi}{30h^2} \cdot \frac{\nu \, \mathrm{d}^2(A/\nu)}{\mathrm{d}\nu^2} \cdot \boldsymbol{F}_{\mathrm{int}}^2, \qquad (1)$$

where $\boldsymbol{F}_{\text{int}} = f \cdot \boldsymbol{F}_{\text{ext}}$, and f is the local field correction factor. In general, f is a tensor quantity and in single crystals this property could be investigated [28,31]. In the following we will treat f as a scalar because the values of electro-optic parameters for single crystals are still at a qualitative level. In the results presented here, the magnitude of the change in dipole moment upon electronic excitation, $|\boldsymbol{\Delta\mu}_{\text{A}}|$, is reported in units of Debye/f to facilitate comparison. This also serves to separate the experimental uncertainty in the derived values of electro-optic parameters from the uncertainties in our knowledge of $\boldsymbol{F}_{\text{int}}$ due to the local field correction factor. In general, for molecules in non-polar environments such as those considered here, f is expected to be somewhat greater than 1.0, but is likely less than 1.3. The angle dependent factor C_χ is given by:

$$C_\chi = 5|\boldsymbol{\Delta\mu}_{\text{A}}|^2 + (3\cos^2\chi - 1) \times \left[3(\boldsymbol{p}\cdot\boldsymbol{\Delta\mu}_{\text{A}})^2 - |\Delta\mu_{\text{A}}|^2\right], \quad (2)$$

where $\boldsymbol{p}$ is the transition moment unit vector which makes an angle ζ_{A} with $\boldsymbol{\Delta\mu}_{\text{A}}$, and χ is the experimental angle between the polarization direction of the probe beam and the applied electric field. The angle ζ_{A} can be obtained by a least-squares fit of ΔA taken at various angles χ to the dependence of $C_\chi / C_{\chi=90°}$ from eq. (2). When $\chi = 54.7°$ (the magic angle), the second term in eq. (2) is zero, and ΔA is proportional simply to $|\boldsymbol{\Delta\mu}_{\text{A}}|^2$. The ν-weighted second derivative is calculated directly from the absorption spectrum using numerical methods; however, for a Gaussian band with a given magnitude (A) and line width (FWHM), the peak value of the second derivative can be approximated by:

$$\nu \frac{\mathrm{d}^2(A/\nu)}{\mathrm{d}\nu^2}(@\nu_{\max}) = \frac{8\ln 2 \cdot A(\nu_{\max})}{(\text{FWHM})^2}. \quad (3)$$

Ideally, electro-absorption data could be obtained with oriented, ultra-thin single crystals, rather than isotropic dispersions of microcrystals or lyophyllized powders. Such experiments are difficult for very strong absorbers such as the chlorophylls. Therefore, in this first report we have studied isotropic dispersions of crystalline materials, although this is less than ideal. An alternative is to study well-defined dimeric systems. Such experiments are reported elsewhere [34]; however, the structural data for even the best characterized synthetic dimers is marginal compared with the high-resolution data for single crystals.

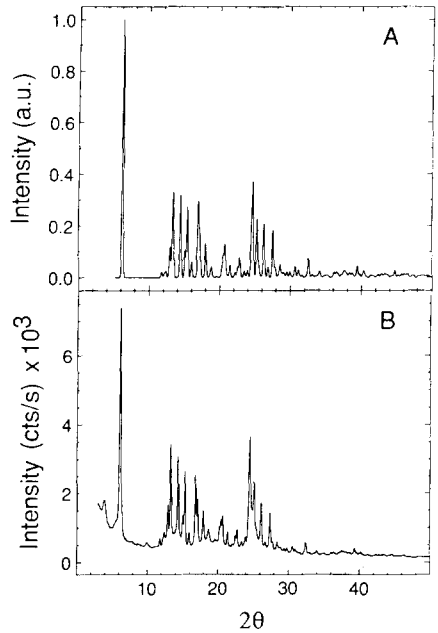

Fig. 2. (a) Simulated powder X-ray diffraction pattern of MePhide a using the crystal structure coordinates [22]; (b) experimental powder X-ray diffraction pattern of lyophilized MePhide a.

3. Results

3.1. Crystallization and X-ray diffraction

The powder X-ray diffraction pattern of lyophyllized MePhide a is shown in fig. 2 and is compared to a synthetic pattern calculated using the MePhide a single crystal coordinates and isotropic thermal parameters (non-H atoms only) [22]. The agreement between the two patterns is quite remarkable and indicates that essentially the same short- and long-range order are present in the powder and a single crystal. This is also

true for pyroMePhide a where lyophyllized and polycrystalline samples produce similar X-ray diffraction patterns (fig. 3). A single crystal structure has not yet been reported for pyroMePhide a, so comparison with a calculated pattern is not possible. Inspection of the patterns reveals that the diffraction of pyroMePhide a is different from that of MePhide a (fig. 2), indicating distinct crystal structures for the two compounds. In particular, the observation that the lowest angle peak occurs at a larger value of 2θ for pyroMePhide a compared to MePhide a indicates a smaller unit cell. This is clear from inspection of the relationship $2\theta_{hkl} = 2\sin^{-1}(\lambda/2d_{hkl})$, i.e. the d-spacing (the spacing between the hkl planes whose diffraction appears at angle 2θ) is inversely related to the diffraction angle.

The results of single crystal X-ray diffraction of MeBacPhide a obtained in the course of this work have been reported elsewhere [24]. Additional attempts to crystallize MeBacPhide a from other solvent mixtures failed to give single crystals with high resolution diffraction [35]. Powder X-ray diffraction results for polycrystalline and lyophyllized MeBacPhide a (fig. 4) are not as definitive as those of the pheophorbides. Neither powder pattern is an identical match of the pattern calculated using the coordinates from the crystal structure [24], although some resemblance is observed in the relative peak positions and intensities. Somewhat better agreement can be obtained by eliminating the coordinates of the benzene molecule of solvation in the synthetic pattern calculation, and this suggests that preparation of the finely ground powder may result in loss of this benzene. Consistent with this hypothesis, we observed that the powder pattern, and hence the overall crystal packing, changes with time (on the order of days) suggesting that the benzene is slowly diffusing from the microcrystals. One further observation from fig. 4 is the difference in the position of the lowest angle peak of the lyophyllized sample compared to the polycrystalline and synthetic patterns. The displacement of the peak to larger 2θ indicates a smaller unit cell as discussed above. In any event,

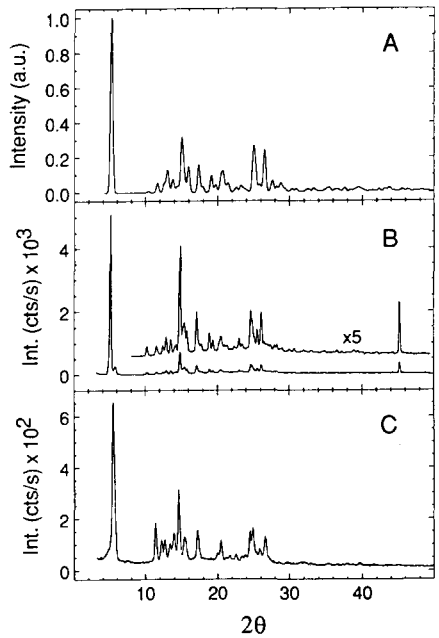

Fig. 4. (a) Simulated powder X-ray diffraction pattern of MeBacPhide a using the crystal structure coordinates [24]; (b) experimental powder X-ray diffraction pattern of polycrystalline MeBacPhide a; (c) experimental powder X-ray diffraction pattern of lyophilized MeBacPhide a.

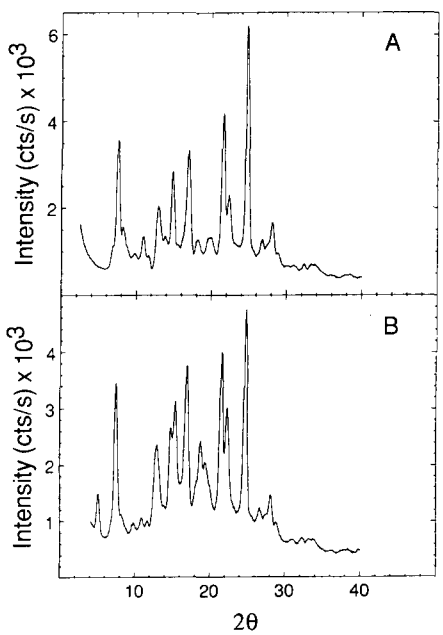

Fig. 3. Powder X-ray diffraction pattern of (a) polycrystalline pyroMePhide a; (b) lyophilized pyroMePhide a.

it is clear that even lyophyllized samples have a large degree of long-range order.

3.2. Absorption and electro-absorption spectroscopy

3.2.1. Methyl pheophorbide a

The absorption and electro-absorption spectra of monomeric MePhide a, including the Soret, Q_x, and Q_y bands are shown in fig. 5. The electro-absorption spectrum of this chromophore is described well by the second derivative of the absorption (compare figs. 5(b) and (c)). This indicates that the dominant effect is a change in dipole moment, $\Delta\mu_A$, upon excitation, with little change in polarizability. The excellent quality of the data allows calculation of the angle ζ_A for the Q_y transition as $23 \pm 2°$. Using this value of ζ_A and the data in fig. 5(b) with eqs. (1) and (2) gives $|\Delta\mu_A| = 1.2 \pm 0.1$ D/f for the $Q_y(0, 0)$ band. Results for the other bands in the visible region are ~ 1.4 D/f and ~ 1.0–1.6 D/f for the Q_x and B bands, respectively. Precise determination of $|\Delta\mu_A|$ for these latter transitions is more difficult due to band overlap and the smaller magnitude of the observed effect. These results are consistent with what one would expect for the difference dipole moment of a moderately symmetric, non-polar molecule in a non-polar matrix.

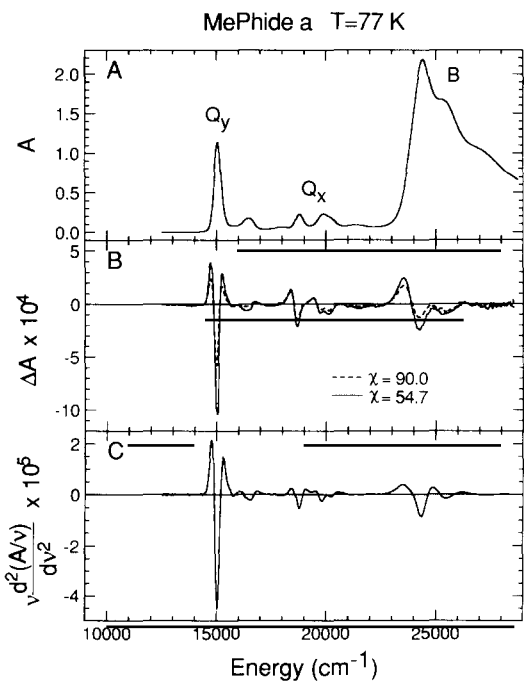

Fig. 5. (a) Absorption, (b) electro-absorption, and (c) second derivative of absorption spectra of monomeric MePhide a in PMMA ($T = 77$ K, $F_{ext} = 5.24 \times 10^5$ V/cm). Electro-absorption spectra are shown for the experimental angles $\chi = 90.0°$ and $\chi = 54.7°$ (magic angle).

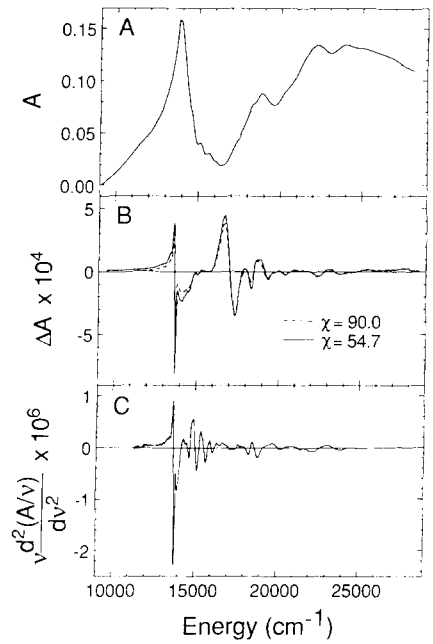

Fig. 6. (a) Absorption, (b) electro-absorption, and (c) second derivative of absorption of lyophilized MePhide a dispersed in PVA ($T = 77$ K, $F_{ext} = 5.89 \times 10^5$ V/cm). Electro-absorption spectra are shown for the experimental angles $\chi = 90.0°$ and $\chi = 54.7°$ (magic angle).

Intermolecular interactions in lyophyllized MePhide a produce very different spectroscopic results compared to the isolated chromophores. Based on the powder diffraction data, we will assume that lyophyllized samples possess the previously determined crystal structure. The absorption and Stark effect spectra of lyophyllized MePhide a in PVA are shown in fig. 6. The Q_y band is red shifted to 725 nm (13 793 cm^{-1}) with a very broad and trailing red edge. One possible explanation for this unusual line shape is that it reflects a heterogeneity in aggregate excitonic interactions. The band maximum would then correspond to the dominant aggregate exciton transi-

tion with a distribution of other aggregates absorbing at lower energy.

The electro-absorption spectrum of lyophyllized MePhide a powder (fig. 6(b)) is similar to the second derivative of the absorption with some significant differences. ΔA for the Q_y band is very large compared to the second derivative and to that of the isolated chromophore, indicating a large dipole moment change; calculation gives $|\Delta\mu_A| = 4.0$–$4.3\ D/f$ with $\zeta_A \sim 49°$. Overlap between the bands in the Q_y region hinders a more precise determination. The most striking difference between the electro-absorption and second derivative spectra is the presence of a large feature centered around 17000 cm^{-1} that does not appear to correspond to either the first (not shown) or second derivative of any feature in the absorption spectrum. The size of this band indicates a substantial change in the electro-optic properties of the electronic states upon excitation. Without a clear line shape from the first and second derivative spectra, it is impossible to tell whether the ΔA line shape is due to a change in the polarizability (first derivative shape) and/or dipole moment (second derivative shape). If the effect is a second derivative shape of some underlying, low intensity absorption band, then the width of this band must be considerable, perhaps as large as 1000 cm^{-1}. Based on data taken at $\chi = 90°$ and 54.7°, ζ_A is approximately 30°–50°, significantly larger than for the isolated monomer Q_y band.

3.2.2. *Pyromethylpheophorbide a*

The electro-absorption spectrum of monomer pyroMePhide a (data not shown) is nearly identical to that of MePhide a shown in fig. 5. The derived value of $|\Delta\mu_A|$ is approximately 1 D/f for the Q_y and Q_x transitions with $\zeta_A \sim 0°$. It is interesting that ζ_A is quite different for monomeric pyroMePhide a and MePhide a. This should present an excellent test for the accuracy of calculations of the properties of simple monomers which must precede the theoretical analysis of more complex systems. Polycrystalline and lyophyllized pyroMePhide a have very similar absorption and electro-absorption spectra; data for lyophyllized pyroMePhide a are presented in fig.

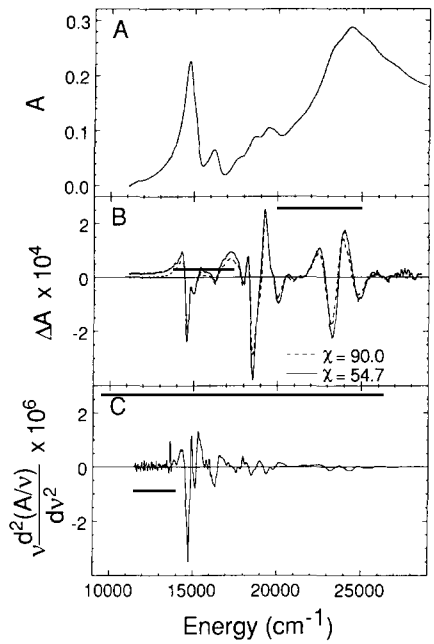

Fig. 7. (a) Absorption, (b) electro-absorption, and (c) second derivative of absorption of lyophilized pyroMePhide a dispersed in PVA ($T = 77$ K, $F_{ext} = 6.09 \times 10^5$ V/cm). Electro-absorption spectra are shown for the experimental angles $\chi = 90.0°$ and $\chi = 54.7°$ (magic angle).

7. The lineshape and red shift of the Q_y band are similar to those observed in MePhide a, but the magnitude of the shift is considerably smaller; the peak maximum appears at 680 nm (14706 cm^{-1}). The electro-absorption spectrum for this aggregate also shows several features with large absorption changes. It is unclear from the absorption spectrum whether these ΔA features correspond to absorption and second derivative features at the same approximate wavelength. Because bands are present, we will assume that the ΔA features do correspond to these bands, and use the measured values required for eqs. (1) and (2). This gives $|\Delta\mu_A|$ values of approximately 2, 8, and 9 D/f for the Q_y, Q_x, and B bands, respectively, for $\zeta_A \sim 40°$. Alternatively, the large features centered around 18500 cm^{-1} and 23200 cm^{-1} may not be due to the Q_x and B transitions at all. Instead, these transitions may be analogous to that at 17000 cm^{-1} in lyphyllized MePhide a, in which case the values of $|\Delta\mu_A|$ are larger still (see discussion below).

3.2.3. Methyl bacteriopheophorbide a

The absorption and electro-absorption spectra of monomeric MeBacPhide a in a PMMA film at 77 K are shown in fig. 8. The electro-absorption spectrum for the Q_y transition, both for the origin at 756 nm (13 228 cm^{-1}) and the first vibronic band approximately 1500 cm^{-1} higher in energy, is well represented by the second derivative of the absorption spectrum. Calculations give $|\Delta\mu_A| = (2.0 \pm 0.1)$ and (1.6 ± 0.2) D/f for the $Q_y(0, 0)$ and $Q_y(0, 1)$ bands, respectively, with $\zeta_A = 16.9° \pm 2°$ for the Q_y origin band. These results are similar to previous measurements of these parameters for bacteriochlorophyll a and bacteriopheophytin a [28,29]. The electro-absorption spectra of the Q_x and Soret regions do not correspond to purely (or predominately) second derivative contributions. The line shapes appear to be dominated by a first derivative contribution (polarizability change with little change in dipole moment); similar results are obtained for these

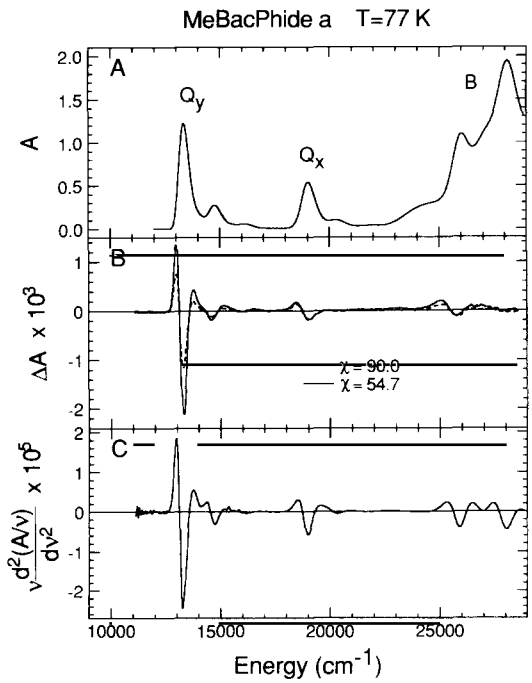

Fig. 8. (a) Absorption, (b) electro-absorption, and (c) second derivative of absorption of monomeric MeBacPhide a in PMMA ($T = 77$ K, $F_{ext} = 5.36 \times 10^5$ V/cm). Electro-absorption spectra are shown for the experimental angles $\chi = 90.0°$ and $\chi = 54.7°$ (magic angle).

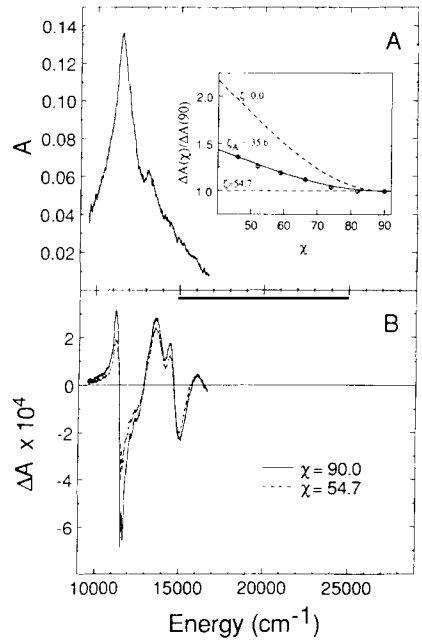

Fig. 9. (a) Absorption and (b) electro-absorption for the near IR region of polycrystalline MeBacPhide a dispersed in PVA ($T = 77$ K, $F_{ext} = 5.54 \times 10^5$ V/cm). Electro-absorption spectra are shown for the experimental angles $\chi = 90.0°$ and $\chi = 54.7°$ (magic angle). The inset in (a) shows the angle dependence for the Stark effect measured at the red-most positive lobe ($\lambda = 890$ nm) to avoid overlap artifacts.

transitions in the spectra of bacteriochlorophyll a and bacteriopheophytin a monomers and in the Q_x region of photosynthetic reaction centers [29].

The absorption and electro-absorption spectra for polycrystalline MeBacPhide a embedded in a PVA matrix are shown in fig. 9. These spectra are much more complicated than those of the isolated chromophore, but at least some qualitative remarks can be made. The absorption of the Q_y region has a similar λ_{max} (867 nm, 11 534 cm^{-1}) to that of the single crystal spectrum taken by Hanson and Hofrichter [25] where $\lambda_{max} = 862$ nm. However, the spectrum of the polycrystalline sample is significantly broader and also has a second, higher energy peak around 13 000 cm^{-1}. The latter is probably a small trace of monomeric MeBacPhide a that is solvated during the film preparation. The larger inhomogeneous broadening, which is similar to that observed in the absorption of lyophyllized MePhide a and py-

roMePhide a discussed previously, may be attributed to the size distribution of micro-crystals and variable amounts of solvent exposure. Because the individual crystalline particles are only several microns (or less) in diameter, there is a significant fraction of the molecules that are solvent-exposed at the interface between the crystal and the matrix. Support for this reasoning comes from a single crystal spectrum taken of the same MeBacPhide a used for the dispersed polycrystalline film and crystallized using the same solvent mixture. This spectrum, obtained using a home-built micro-spectrophotometer whose design is similar to that used by Hanson and Hofrichter [25], reproduces their spectrum in λ_{max} and line shape (data not shown).

The electro-absorption spectrum of polycrystalline MeBacPhide a (fig. 9(b)) is similar to that for the other pheophorbides in that there is a very strong effect on the Q_y transition and the presence of other, electric field-enhanced bands not discernible in the absorption spectrum. In this case, a band appears at 15000 cm^{-1} that does not seem to correspond to any absorption feature. The absorption data are not of sufficient quality to obtain reliable second derivatives; however, using an estimate of the bandwidth (FWHM = 1500 cm^{-1}) to approximate the magnitude of the second derivative at the peak of the Q_y band (eqn. (3)) results in $|\Delta\mu_A| \sim 12$ D/f, using the angle dependence shown in the inset to fig. 9.

4. Discussion

4.1. Powder X-ray diffraction

The results presented here indicate that powder X-ray diffraction may be a generally useful method for characterizing the structures of complex chromophore aggregates in the absence of large single crystals and under conditions which may sometimes be more useful for absorption spectroscopy. One of the most striking observations made during the course of this investigation was the difficulty of preparing truly amorphous (i.e. disordered) powders of chlorophyll chromophores. In some cases lyophyllized powders dried from benzene show the same crystal packing as carefully grown single crystals. There appears to be a natural tendency for these molecules, perhaps because of their plate-like structure, to align themselves with a particular long-range order. Based on this data, we adopt the working hypothesis that polycrystalline and lyophyllized powders have the local and long-range structure of a macroscopic crystal. It is interesting that BChl d crystals grown under different conditions resulted in different structures [46]. Within the range of conditions tested here, this does not appear to be the case for MePhide a or pyroMePhide a.

4.2. Absorption and electro-absorption spectra

The high quality electro-absorption spectra of the monomeric chromophores in figs. 5 and 8 should provide a precise target for spectral simulations. The dipole moment differences are generally quite small. In addition there is little evidence for a first derivative contribution to ΔA of the Q_y transition, consequently changes in polarizability upon Q_y excitation are very small. This result is typical for aromatic molecules with fairly low symmetry, and contrasts sharply with the conjugated polyenes [47–49].

Although the absorption and electro-absorption data for polycrystalline and lyophyllized samples are still far from ideal, several consistent trends emerge. Ideally, one would like to have identical local structures in order to analyze such trends without resorting to detailed calculations, but small variations in the local structure from one system to another, specifically in the intermolecular spacing, make this rather difficult. As discussed at the outset, variations of less than 0.1 Å in the intermolecular spacing and the offset between macrocycles can have a substantial effect on the spectral properties.

The red shift of the Q_y transition observed in all of the pheophorbide aggregate absorption spectra is similar to that of many other aggregates including several chlorophyllide polycrystalline samples [50], evaporated thin films of BPheo a [51], mixed aqueous-organic solvent formed oligomers of BChl and BPheo [52], and antennas

and RCs of photosynthetic bacteria [33]. The origin of the shift in MeBacPhide a crystals, according to the analysis of Hanson and Hofrichter, are the π–π interactions between the porphyrin rings which form one-dimensional stacks and two-dimensional layers [25]. They base their conclusion on the fact that, since no Mg is present in MeBacPhide a and the single crystal is a water-free environment, no hydrogen bonding can occur. Hydrogen bonding and axial ligation had been proposed as some of the causes of the large red shifts observed in aggregate chromophore complexes [50].

The present work is consistent with the notion that the magnitude of the Q_y red shift is an indication of the strength of the intermolecular interactions. This strength is reflected in the difference dipole between the ground state and the excited state. $|\Delta\mu_A|$, assuming the ground state dipole is small, is a measure of the polar character of the excited state and is an indicator of mixing with nearby CT states. Simulations by Parson et al. [5] of the electronic absorption for crystalline MeBacPhide a indicate the presence of a number of CT transitions that should be in the visible and near IR regions of the spectrum and which correspond to electron transfers from an origin molecule to its nearest neighbors. The calculations in ref. [5] used the earlier, low precision coordinates of the crystal structure [23]. Professor Parson kindly provided the program used in ref. [5], and the absorption spectrum was recalculated using the updated X-ray diffraction determined atomic coordinates [24]. The results highlight the extreme sensitivity of the spectral simulations to small changes in the coordinates. First, electrostatic calculations reveal a 200 cm^{-1} difference in the energies of the CT states determined using the different coordinates. Second, in order to maintain the Q_y transition at the experimentally measured energy [25], the CT transitions needed to be adjusted an additional 2000 cm^{-1} higher in energy. The precise origins of this difference in terms of meaningful theoretical factors are hard to pinpoint, as there are many assumptions and approximations implicit in the calculation (see ref. [54] for extensive discussion of these issues). It is remarkable that very small changes in the atomic coordinates lead to changes in the calculated energies of CT states of the order of 2000 cm^{-1} (250 meV). Such differences in structure would go undetected at the current level of resolution of reaction center structures [17–20], therefore it is unclear whether calculated spectra based on these protein structures can be quantitatively interpreted at this time. Furthermore, it is uncertain that the protein X-ray structure refinement will ever progress to the level where such structurally subtle, but electronically significant, differences can be reliably determined.

In all cases we find that the change in dipole moment associated with the red-shifted Q_y bands in these aggregates is substantially larger than in the corresponding monomer. This is what is observed in RCs [28–32] and in some antenna complexes [33]. In most cases, and in contrast with the natural systems, new transitions are observed in the electro-absorption spectra of the crystalline samples which are not obviously present in the absorption spectra. It is reasonable to suggest that these may be inter-molecular charge-transfer transitions. The presence of CT transitions in the visible region is predicted from calculations on MeBacPhide a crystals [5] as discussed in the previous paragraph. Such transitions have been observed in Stark spectra of thin films of crystalline aromatic hydrocarbons (e.g. tetracene, pentacene) [37–40] and phthalocyanines [41], and their properties have been described theoretically [54]. Because of the close energetic proximity of these transitions to locally excited $\pi\pi^*$ and exciton transitions, we expect that there will be strong mixing among these transitions. Thus, although these transitions are identified with CT states, the precise degree of CT character is not easy to specify. It should be noted, however, that in contrast with most intermolecular systems studied to date, the underlying absorption associated with these strong ΔA signals is very weak. This makes it very difficult to quantify the value of $|\Delta\mu_A|$, as this relies on a comparison with the second derivative of the absorption. The fact that ζ_A is substantially larger in all aggregates than for the parent monomers is especially interesting and parallels what is observed in the reaction center [28–32]. This is consistent with the notion that

the dipolar state which is mixed into the lowest Q_y transition lies out of the plane of the macrocycle, as would be expected for a contribution from an inter-molecular CT state. Of course, the angle ζ_A only defines a cone, not a single direction in space, so we can at best present a consistency argument as is always true with dichroism data. Finally, if these new bands are due to CT transitions, then the higher energy of the new band in the pyrolyzed chromophore is consistent with redox potential measurements of the two molecules in solution [43,53]. Simple arguments, based solely on the redox potentials, would predict a higher energy CT state in pyroMePhide a than in MePhide a.

Recently we have examined the electro-absorption spectrum of the special pair in photosynthetic RCs at 1.5 K in glassy matrices where the inhomogeneous line width is substantially narrower [55]. Under these conditions, a discrepancy between the electro-absorption spectrum and the second derivative of the absorption spectrum can be observed. The results indicate that a substantial first derivative contribution is present corresponding to a change in polarizability. Further consideration of the consequences of mixing with CT states suggests that the excited state of the special pair is best described as a highly polarizable state, with the substantial observed dipole moment being induced by the organized matrix field in the RC. This is analogous to the situation for polarizable polyenes in antenna [49,56] and RC [56] complexes. The crystalline aggregates studied here likewise should have regular, ordered matrix fields; however, the magnitude of the induced contribution cannot be assessed because it has thus far proven difficult to extract reliable polarizabilities from the data. To date, attempts to calculate the electronic and electro-optic properties of photosynthetic pigment complexes have not considered these factors which are likely to be very important.

In summary, the low-lying electronic transitions of aggregates of the photosynthetic pigments are found to be substantially more sensitive to an applied electric field than these transitions in the corresponding monomeric pigments. This is interpreted as an increase in dipolar character due to mixing with charge transfer states involving one-electron oxidation and reduction of the neighboring macrocycles. These dipolar properties correlate with the red shift of the lowest energy absorption maxima. The measured direction of charge displacement is always substantially larger in the aggregates than in the monomers, again consistent with mixing of states whose dipole moment lies out-of-plane. Ideally, these experiments should be performed on single crystals; however, this is a difficult experiment. Even though the dispersed aggregates often have complex absorption spectra the general trends discussed above appear to be reliable indicators of inter-chromophore interactions.

Acknowledgements

X-ray powder diffraction data were obtained at the Stanford Center for Materials Research supported by NSF Grant DMR90-22248, or at Scintag Corp., Santa Clara, California with the kind assistance of Dr. Lawrence Bernstein. Dr. Louise Hanson kindly shared samples of methylbacteriopheophorbide a single crystals and crystallization methodology with us. We also acknowledge extensive discussions with Professor W. Parson concerning the calculations reported in ref. [5] and with Dr. Jack Fajer. D.S.G. was an NSF Predoctoral and GAANN Fellow. This work was supported in part by grants from the National Science Foundation.

References

[1] R.M. Pearlstein and R.P. Hemenger, Proc. Natl. Acad. Sci. USA 75 (1978) 4920.
[2] R.M. Pearlstein, in: Organization and Function of Photosynthetic Antennas, eds. H. Scheer and S. Schneider (Walter de Gruyter, Berlin, 1988) p. 555.
[3] A. Warshel and W.W. Parson, J. Am. Chem. Soc. 109 (1987) 6143.
[4] S. Creighton, J.-K. Hwang, A. Warshel, W.W. Parson and J. Norris, Biochemistry 27 (1988) 774.
[5] W.W. Parson, S. Creighton and A. Warshel, J. Am. Chem. Soc. 111 (1989) 4277.
[6] J. Eccles, B. Honig and K. Schulten, Biophys. J. 53 (1988) 137.

[7] H. Scheer, ed., Chlorophylls (CRC Press, Boca Raton, 1991).
[8] M.E. Michel-Beyerle, ed., Antennas and Reaction Centers of Photosynthetic Bacteria (Springer, Berlin, 1985).
[9] J. Breton and A. Vermeglia, eds., The Photosynthetic Bacterial Reaction Center – Structure and Dynamics (Plenum, New York, 1988) p. 151.
[10] M.E. Michel-Beyerle, ed., Reaction Centers of Photosynthetic Bacteria, Springer Series in Biophysics, Vol. 6 (Springer, Berlin, 1990).
[11] R. Moog, A. Kuki, M.D. Fayer and S.G. Boxer, Biochemistry 23 (1984) 1564.
[12] M. Kasha, Radiation Res. 20 (1963) 55.
[13] M. Kasha, H.R. Rawls and M.A. El-Bayoumi, Pure Appl. Chem. 11 (1965) 371.
[14] R.M. Pearlstein, in: Photosynthesis - Energy Conversion by Plants and Bacteria, ed. Govindjee (Academic Press, New York, 1982) p. 293.
[15] See for example ref. [7], Ch. 4.9, 4.10, 4.11 and 4.12.
[16] J. Deisenhofer, O. Epp, K. Miki, R. Huber and H. Michel, J. Mol. Biol. 180 (1984) 385.
[17] J. Deisenhofer, O. Epp, K. Miki, R. Huber and H. Michel, Nature 318 (1985) 618.
[18] J.P. Allen, G. Feher, T.O. Yeates, H. Komiya and D.C. Rees, Proc. Natl. Acad. Sci. USA 84 (1987) 5730.
[19] J.P. Allen, G.Feher, T.O. Yeates, H. Komiya and D.C. Rees, Proc. Natl. Acad. Sci. USA 84 (1987) 6162.
[20] C.H. Chang, D. Tiede, J. Tang, U. Smith, J.R. Norris and M. Schiffer, FEBS Lett. 205 (1986) 82.
[21] K.M. Barkigia, L. Chantranupong, K.M. Smith and J. Fajer, J. Am. Chem. Soc. 110 (1988) 7566.
[22] M.S. Fischer, D.H. Templeton, A. Zalkin and M. Calvin, J. Am. Chem. Soc. 94 (1972) 3613.
[23] K.M. Barkigia, J. Fajer, K.M. Smith and G.J.B. Williams, J. Am. Chem. Soc. 103 (1981) 5890.
[24] K.M. Barkigia, D.S. Gottfried, S.G. Boxer and J. Fajer, J. Am. Chem. Soc. 111 (1989) 6444.
[25] L.K. Hanson and J. Hofrichter, Photochem. Photobiol. 41 (1985) 247.
[26] S.G. Boxer, R.A. Goldstein, D.J. Lockhart, T.R. Middendorf and L. Takiff, J. Chem. Phys. 93 (1989) 8280.
[27] L.M. McDowell, C. Kirmaier and D. Holten, Biochim. Biophys. Acta 1020 (1990) 239.
[28] D.J. Lockhart and S.G. Boxer, Biochemistry 26 (1987) 664, 2958.
[29] D.J. Lockhart and S.G. Boxer, Proc. Natl. Acad. Sci. USA 85 (1988) 107.
[30] T.R. Middendorf, L. Mazzola and S.G. Boxer, submitted.
[31] M. Lösche, G. Feher and M.Y. Okamura, Proc. Natl. Acad. Sci. USA 84 (1987) 7537.
[32] M. Lösche, G. Feher and M.Y. Okamura, in: The Photosynthetic Bacterial Reaction Center – Structure and Dynamics, eds. J. Breton and A. Vermeglia (Plenum, New York, 1988).
[33] D.S. Gottfried, J.W. Stocker and S.G. Boxer, Biochim. Biophys. Acta 1059 (1991) 63.
[34] T.R. Middendorf, D.S. Gottfried, D.J. Lockhart, D. Johnson, M. Wasielewski and S.G. Boxer, in preparation.
[35] D.S. Gottfried, Ph.D. Thesis, Stanford University (1990).
[36] S. Krawczyk, Biochim. Biophys. Acta 1056 (1991) 64.
[37] L. Sebastian, G. Weiser and H. Bässler, Chem. Phys. 61 (1981) 125.
[38] L. Sebastian, G. Weiser, G. Peter and H. Bässler, Chem. Phys. 75 (1983) 103.
[39] B. Petelenz, P. Petelenz, H.F. Shurvall and V.H. Smith, Jr., Chem. Phys. Lett. 133 (1987) 157.
[40] P. Petelenz, W. Siebrand and M.Z. Zgierski, Chem. Phys. Lett. 147 (1988) 430.
[41] H. Yoshida, Y. Tokura and T. Koda, Chem. Phys. 109 (1986) 375.
[42] K.M. Smith, D.A. Goff and D.J. Simpson, J. Amer. Chem. Soc. 107 (1985) 4946.
[43] R.R. Bucks, Ph.D. Thesis, Stanford University (1982).
[44] W. Liptay, in: Excited States, Vol. 1, ed. E.C. Lim (Academic Press, New York, 1974) p. 129.
[45] R.A. Mathies, Ph.D. Thesis, Cornell University (1974).
[46] J. Fajer, K.M. Barkigia, E. Fujita, D.A. Goff, L.K. Hanson, J.D. Head, T. Horning, K.M. Smith and M.C. Zerner, in: Antennas and Reaction Centers of Photosynthetic Bacteria, ed. M.E. Michel-Beyerle (Springer, Berlin, 1985) p. 324.
[47] M. Ponder and R. Mathies, J. Phys. Chem. 87 (1983) 5090.
[48] W. Liptay, R. Wortmann, R. Bohm and N. Detzer, Chem. Phys. 120 (1988) 439.
[49] D.S. Gottfried, M.A. Steffen and S.G. Boxer, Science 251 (1991) 662.
[50] C. Kratky and J.D. Dunitz, J. Mol. Biol. 113 (1977) 431.
[51] A.A. Krasnovskii, M.I. Bystrova and A.V. Unrikhina, Dokl. Akad. Nauk SSSR 235 (1977) 232.
[52] A. Scherz and W.W. Parson, Biochim. Biophys. Acta 766 (1984) 653.
[53] R.R. Bucks, I. Fujita, T.L. Netzel and S.G. Boxer, J. Phys. Chem. 86 (1982) 1947.
[54] P.J. Bounds and W. Siebrand, Chem. Phys. Lett. 75 (1980) 414.
P.J. Bounds, P. Petelenz and W. Siebrand, Chem. Phys. 63 (1981) 303.
P.J. Bounds and W. Siebrand, Chem. Phys. Lett. 85 (1982) 496.
[55] T.R. Middendorf, Ph.D. Thesis, Stanford University (1991).
[56] D.S. Gottfried, M.A. Steffen and S.G. Boxer, Biochim. Biophys. Acta. 1059 (1991) 76.